Imaging tuberculosis with endogenous β-lactamase reporter enzyme fluorescence in live mice

Ying Kong[a], Hequan Yao[b,1], Hongjun Ren[b,1], Selvakumar Subbian[a,1,2], Suat L. G. Cirillo[a], James C. Sacchettini[c], Jianghong Rao[b,3], and Jeffrey D. Cirillo[a,3]

[a]Department of Microbial and Molecular Pathogenesis, Texas A&M Health Sciences Center, College Station, TX 77843; [b]Molecular Imaging Program at Stanford, Departments of Radiology and Chemistry, Stanford University, Stanford, CA 94305; and [c]Departments of Chemistry and Biochemistry and Biophysics, Texas A&M University, College Station, TX 77843

Edited by Rino Rappuoli, Novartis Vaccines, Siena, Italy, and approved June 4, 2010 (received for review January 17, 2010)

The slow growth rate and genetic intractability of tubercle bacilli has hindered progress toward understanding tuberculosis, one of the most frequent causes of death worldwide. We overcame this roadblock through development of near-infrared (NIR) fluorogenic substrates for β-lactamase, an enzyme expressed by tubercle bacilli, but not by their eukaryotic hosts, to allow real-time imaging of pulmonary infections and rapid quantification of bacteria in living animals by a strategy called reporter enzyme fluorescence (REF). This strategy has a detection limit of $6 \pm 2 \times 10^2$ colony-forming units (CFU) of bacteria with the NIR substrate CNIR5 in only 24 h of incubation in vitro, and as few as 10^4 CFU in the lungs of live mice. REF can also be used to differentiate infected from uninfected macrophages by using confocal microscopy and fluorescence activated cell sorting. *Mycobacterium tuberculosis* and the bacillus Calmette–Guérin can be tracked directly in the lungs of living mice without sacrificing the animals. Therapeutic efficacy can also be evaluated through loss of REF signal within 24 h posttreatment by using in vitro whole-bacteria assays directly in living mice. We expect that rapid quantification of bacteria within tissues of a living host and in the laboratory is potentially transformative for tuberculosis virulence studies, evaluation of therapeutics, and efficacy of vaccine candidates. This is a unique use of an endogenous bacterial enzyme probe to detect and image tubercle bacilli that demonstrates REF is likely to be useful for the study of many bacterial infections.

infection | pulmonary | *Mycobacterium* | fluorogenic | beta-lactamase

Tuberculosis, caused by *Mycobacterium tuberculosis* (Mtb), remains one of the most frequent causes of death in humans worldwide by killing nearly 2 million people each year (1). Emergence of strains resistant to multiple drugs has led to situations where treatment is no better than before the discovery of antibiotics (2, 3). Diagnosis of tuberculosis remains a major barrier to control of the disease because the standard method, the acid-fast smear using sputum, does not become positive until a few months after transmission occurs. Culture-based techniques are more sensitive, but still take weeks to obtain results. Similar problems plague tuberculosis research in general, and particularly in animal models, where data from assays is dependent upon determination of colony-forming units (CFU). This problem impacts the pace of virulence studies, evaluation of therapeutics, and development of vaccines. All tuberculosis research and diagnosis would be facilitated by methods to detect tubercle bacilli in vitro and during disease. Although recombinant reporter strains of mycobacteria have been developed for detection of mycobacteria using fluorescence, luminescence (4–8), and even single photon emission computed tomography (SPECT) (9, 10), these methods require specific laboratory strains and do not allow detection of pulmonary tuberculosis by optical imaging directly in live animals. Recombinant systems have facilitated progress, but expression of a foreign gene can impact bacterial fitness in unexpected ways, particularly when expressed from plasmids (11–13). The ability to detect all strains that cause tuberculosis directly without expression of foreign genes would have a profound impact upon the tuberculosis field and would facilitate research with clinical strains that cause tuberculosis. Sensitive detection of nonrecombinant strains that cause tuberculosis can also improve clinical diagnosis using sputum and other diagnostic samples as well as ultimately be applied directly to diagnosis of infections in patients.

We describe noninvasive detection of natural strains that cause pulmonary tuberculosis in living animals. Detection is based on reporter enzyme fluorescence (REF) technology, which uses β-lactamase, a naturally occurring enzyme expressed by Mtb (14, 15), as the reporter enzyme and unique fluorogenic substrate probes for imaging. Although optical probes for endogenous enzymes have been used to differentiate cancerous tissue from normal tissue in the field of oncology (16), they have not been used for infectious diseases where, due to the presence of enzymatic targets that are unique to pathogens, this approach has the potential for exquisite specificity. A great deal is known about β-lactamase enzymes and substrates because they are the most common mechanism of bacterial resistance to penicillin and cephalosporin antibiotics through hydrolysis of a β-lactam ring (17–20). Comparison of the crystal structure of the Mtb β-lactamase, BlaC, to that of other similar enzymes, such as the *Escherichia coli* β-lactamase TEM-1, reveals that BlaC has an unusually large active site pocket, suggesting that design of substrates with high specificity should be straightforward (21). Considering that catalytic reporters can produce a measurable signal at 1,000-fold lower protein levels than fluorescent proteins (22), β-lactamase REF has the potential for extremely high sensitivity. These characteristics, along with the very high catalytic activity (23) of β-lactamase, make this enzyme a nearly ideal choice for development of specific probes to detect tuberculosis in the laboratory, live animals, or patients.

Results

Expression of β-Lactamase by Mtb. We evaluated the expression of β-lactamase in different strains that cause tuberculosis. All strains of Mtb examined express BlaC at levels measurable within 2 h and increasing in signal intensity to 20 h (Fig. 1*A*). As expected, a specific mutant in Mtb *blaC* (24) produces greater than 10-fold lower levels of signal, indicating that BlaC is responsible for the

Author contributions: J.R., and J.D.C. designed research Y.K., H.Y., H.R., S.S., S.L.G.C., J.R., and J.D.C. performed research; Y.K., H.Y., H.R., J.C.S., J.R., and J.D.C. contributed new reagents/analytic tools; Y.K., H.Y., H.R., S.S., S.L.G.C., J.C.S., J.R., and J.D.C. analyzed data; and Y.K., S.S., S.L.G.C., J.R., and J.D.C. wrote the paper.

The authors declare no conflict of interest.

This article is a PNAS Direct Submission.

Freely available online through the PNAS open access option.

[1]H.Y., H.R., and S.S. contributed equally to this work.

[2]Present address: W250T, Public Health Research Institute at University of Medicine and Dentistry of New Jersey, 225 Warren St., Newark, NJ 07103.

[3]To whom correspondence may be addressed. E-mail: jdcirillo@medicine.tamhsc.edu or jrao@stanford.edu.

This article contains supporting information online at www.pnas.org/lookup/suppl/doi:10.1073/pnas.1000643107/-/DCSupplemental.

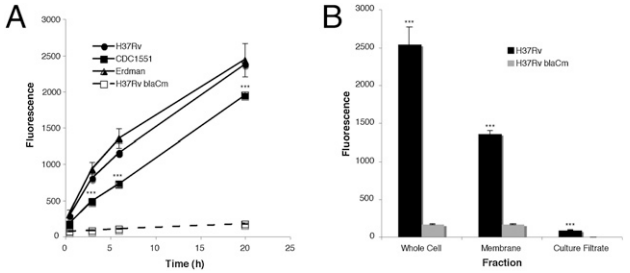

Fig. 1. *Mycobacterium tuberculosis* (Mtb) strains produce a membrane-localized β-lactamase. (*A*) The three common laboratory Mtb strains H37Rv, CDC1551, and Erdman all produce similar levels of β-lactamase as measured by the change in fluorescence of Fluorocillin Green (excitation: 485 nm; emission: 530 nm) in the presence of 10^7 bacteria. In the case of CDC1551, the signal produced is significantly lower (***$P < 0.001$) than Erdman and H37Rv, yet it is at least 10-fold higher than background. The H37Rv blaCm strain with a mutation in the *blaC* gene displays negligible β-lactamase activity. (*B*) Membrane fractions of Mtb are responsible for the majority of the β-lactamase activity found in whole-cell fractions, suggesting that BlaC is primarily membrane-localized in Mtb. β-Lactamase levels in culture filtrates are significantly higher than background ($P < 0.001$), indicating that BlaC is secreted at low levels.

majority of β-lactamase activity in Mtb. The Mtb BlaC is primarily surface-localized because membrane fractions carry the majority of the activity (Fig. 1*B*). The fact that the Mtb BlaC is surface-localized makes it a nearly ideal candidate for use to detect Mtb because substrates would not have to traverse the bacterial cell wall. This is a significant issue for detection of mycobacteria because their cell wall is thought to be highly selective.

Substrates for Detection of Mtb β-Lactamase. We have developed substrates that are eukaryotic cell permeable and produce a long wavelength fluorescent signal when cleaved that is amenable to use in live animal imaging due to the ability of long wavelengths to penetrate mammalian tissue efficiently (25, 26). To detect Mtb using BlaC, we designed several near-infrared fluorogenic substrates: CNIR4, CNIR5, CNIR9, and CNIR10 (Fig. S1*a*). These "molecular switches" or "beacons" are not fluorescent before cleavage due to the presence of a quencher, QSY21 or its derivative, linked to either Cy5 (CNIR4) or Cy5.5 (CNIR5, CNIR9, and CNIR10) through a lactam ring, leading to a fluorescence resonance energy transfer (FRET) quenching effect (Fig. 2). BlaC cleavage triggers spontaneous fragmentation, releasing the quencher connected to the 3′ position of the lactam, breaking the FRET process, and restoring fluorescence emission. The quencher QSY21 was modified to make a hydrophilic QSY21 disulfonate that absorbs maximally at 649 nm and a hydrophobic QSY22 that absorbs maximally at 670 nm to allow optimal quenching of Cy5 and Cy5.5, respectively. We connected acetylated D-glucosamine to the carboxylate of cysteine through a γ-amino-butyric acid as the linker in CNIR5 and CNIR9 because we have shown that fully acetylated glucosamine can facilitate uptake of the highly charged CNIR4 into eukaryotic cells

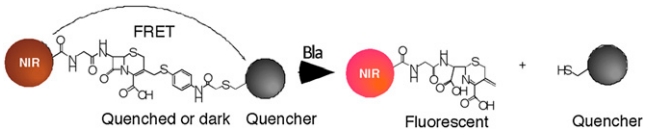

Fig. 2. Reporter enzyme fluorescence detection of *M. tuberculosis* with near-infrared (CNIR) fluorogenic substrates. The intact CNIR substrates do not display fluorescence due to the close proximity of the fluorescent dye (Cy5 or Cy5.5) and the quencher through fluorescence resonance energy transfer (FRET), but become fluorescent after hydrolysis by β-lactamase, generating the fluorescent product whose emission can be measured using a fluorometer. The quencher groups used are QSY21 or derivatives and the CNIR dyes are Cy5 (CNIR4) and Cy5.5 (CNIR5, CNIR9, and CNIR10). NIR, near-infrared.

(25). We designed CNIR10 without the D-glucosamine to directly evaluate the impact of a smaller, less charged probe. All four probes display little fluorescence before β-lactamase cleavage and an increase in maximal emission by 8.5- (660 nm, CNIR4), 24- (690 nm, CNIR5), 9.5- (690 nm, CNIR9), and 10-fold (690 nm, CNIR10) after cleavage (Fig. S1*b*). We found that coincubation of each of these probes with Mtb resulted in direct labeling of the bacteria, with an increase in fluorescence of 2-fold for CNIR4, 3-fold for CNIR5, 1.5-fold for CNIR9, and 2-fold for CNIR10 after 18 h coincubation (Fig. S1*C*).

Detection and Quantification of Mtb in Vitro. In the case of CNIR5, which displays the greatest increase in fluorescence during coincubation with Mtb, we found a good correlation ($r^2 = 0.989$) between bacterial numbers and level of fluorescence over a broad range of bacteria from 10^2 to 10^6 colony forming units (Fig. 3*A*). The calculated limit of detection using CNIR5 was $6 \pm 2 \times 10^2$ CFU. The calculated limit of detection using CNIR5 for other β-lactamase–producing bacteria was similar: $6 \pm 1 \times 10^2$ CFU for *Pseudomonas aeruginosa* and $8 \pm 0.7 \times 10^2$ CFU for *Staphylococcus aureus*. Incorporation of the fluorescent dye into Mtb was confirmed by fluorescence confocal microscopy at 24 h coincubation whereas Mtb in the absence of CNIR does not display fluorescence at 690 nm (Fig. 3*B*). Mtb within macrophages could also be detected with CNIR, and there is a good correlation ($r^2 = 0.984$) between bacterial numbers and fluorescence intensity (Fig. 3*C*), with a threshold of detection of 1–5 × 10^5 bacteria. Interestingly, the most intense staining with all four CNIR substrates is within compartments in the cytoplasm of macrophages, suggesting that these substrates efficiently penetrate subcellular compartments and that the majority of the active Mtb BlaC is accessible to substrate outside of the bacteria (Fig. 3*D*), which is consistent with our fractionation studies. CNIR labeling allows direct detection of infected versus uninfected macrophages using microscopy, a useful tool for studies with tissue culture cells. Cytotoxicity of these substrates was examined as described previously (27) in J774A.1 cells, and no significant cytotoxicity occurs with concentrations up to 100-fold higher than those used for detection of Mtb. We also found that CNIR can be used to differentiate infected from uninfected cells by fluorescence-activated cell sorting (FACS; Fig. 3*E*), making it possible to quantify infected cells during in vitro studies or in homogenized tissues from animal studies. The number of cells separated by FACS using either recombinant green fluorescent protein (GFP) or CNIR was similar and correlated with the multiplicity of infection (MOI) used.

Real-Time Analysis of Tuberculosis in Living Animals. These observations indicate that Mtb can be detected and quantified using REF, but do not address whether CNIR will allow detection directly in animals. To establish the kinetics of CNIR substrates for quantification of Mtb in mammalian tissues, we infected BALB/c mice by s.c. inoculation with Mtb and the closely related vaccine strain bacillus Calmette–Guérin. We found that CNIR4, CNIR5, CNIR9, and CNIR10 could detect 10^7 s.c. bacteria and CNIR5 could readily detect 10^6 bacteria (Fig. 4). Maximal fluorescence is observed at 48 h postadministration of the substrate with CNIR5 producing the highest levels of signal followed by CNIR10, CNIR4, and CNIR9. Fluorescent signal is not significantly different from background for any substrate after 96 h postadministration, allowing the substrate to be readministered to the same animals for subsequent imaging. Both bacillus Calmette–Guérin- and Mtb-infected animals display nearly identical kinetics and signal strength with all CNIR substrates. The improved signal observed for CNIR5 over CNIR4 is most likely due to the beneficial characteristics of the longer wavelength of excitation and emission for Cy5.5 over Cy5, but the lower signals of CNIR9 and CNIR10 are likely the result of differences in their membrane

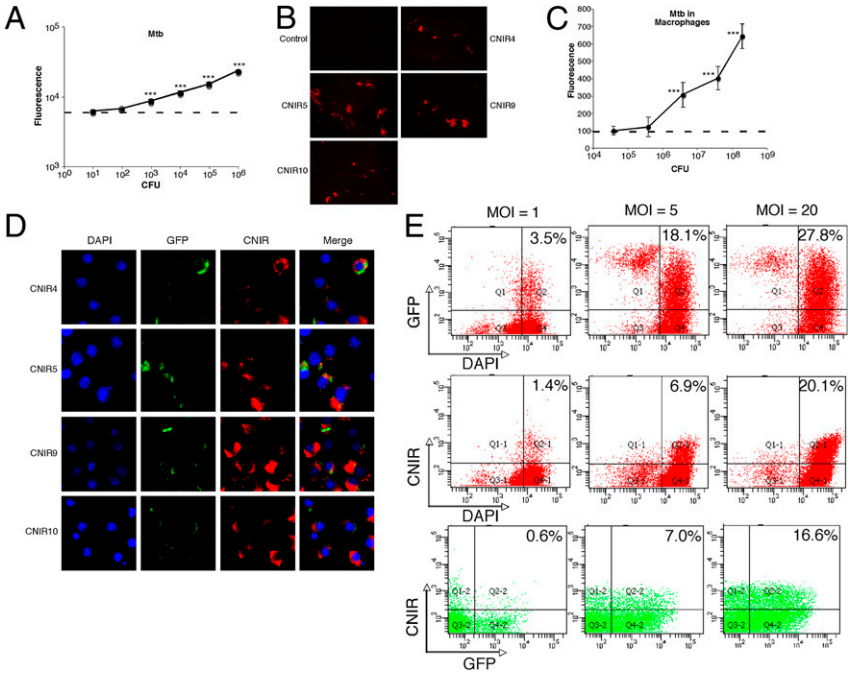

Fig. 3. Fluorogenic compounds allow detection of *M. tuberculosis* (Mtb) in vitro and direct detection of infected cells by confocal microscopy and fluorescence activated cell sorting (FACS). (*A*) Correlation of fluorescent signal and number of tubercle bacilli in culture as determined by colony-forming units (CFU) in the presence of CNIR5 for 24 h. (*B*) Fluorescence confocal microscopy of Mtb coincubated with the CNIR substrates for 24 h demonstrates fluorescence incorporation into the bacteria. (*C*) Correlation of fluorescent signal and number of tubercle bacilli present within J774A.1 murine macrophages after coincubating with CNIR5 for 24 h. (*D*) Fluorescence confocal microscopy of J774A.1 murine macrophages infected with GFP (green) expressing Mtb and coincubated with CNIR substrates (red) for 24 h. Fixed cells were stained with DAPI (blue) to visualize nuclei. Infected cells can be identified by the presence of signal from CNIR substrates whereas uninfected cells do not incorporate CNIR signal. (*E*) FACS allows separation of infected J774A.1 murine macrophages labeled with CNIR5 in a manner that correlates well with the multiplicity of infection (MOI) bacteria per cell. Separation can be accomplished with GFP, GFP-expressing Mtb, or CNIR or by using both fluorescent labels. $***P < 0.001$: significantly different from fluorescence of medium alone (horizontal dashed lines in *A* and *C*) calculated by ANOVA with the Bonferroni posttest.

permeability. This conclusion is supported by the lower incorporation of fluorescence into the bacteria over time observed for both CNIR9 and CNIR10 compared with CNIR5 (Fig. S1*C*). Although acetylated glucosamine improves uptake of these substrates, the sulfates also play an unexpected role in improving the observed imaging kinetics that cannot be compensated for by the lower molecular weight of CNIR10.

Localization and Quantification of Pulmonary Infection. Pulmonary infection is the natural route of infection by Mtb, but the greater tissue depth and complexity of the lung make detection more difficult. We infected mouse lungs with bacillus Calmette–Guérin and Mtb and imaged them by transillumination after administration of CNIR5 for REF. At both 24 and 48 h postadministration of CNIR5, as few as 10^4 CFU could be detected in the lungs of living mice (Fig. 5 *A* and *C*). Although the signal correlates well with bacterial numbers at 24 h, the levels of signal equalize by 48 h postadministration of CNIR5, suggesting that the fluorophore builds up at the site of infection, consistent with pooling of fluorophore in the cytoplasm of infected macrophages. Lung examined ex vivo at 48 h displays a strong signal from infected animals but no signal from uninfected animals, demonstrating that the source of the signal is clearly within infected lungs (Fig. 5*D*). Localization of the source of the signal from CNIR5 was confirmed by 3D fluorescence-mediated molecular tomography (FMT) analyses in living mice (Fig. S2). FMT of animals at 24 and 48 h consistently localizes the signal source within the lungs and allows accurate quantification of the concentration of the fluorochrome, as shown by the nearly linear correlation with the number of bacteria present (Fig. S2*D*; $r^2 = 0.863$). We calculated the limit of detection for live animal imaging using REF in mice after pulmonary infection to be $1.3 \pm 0.6 \times 10^4$ CFU. Because adult human lung attenuates near-infrared signals approximately 10-fold for every 2.5 cm of depth (28, 29) and the sensitivity of REF optical imaging allows detection of low bacterial numbers ($\sim 10^4$ CFU) within lung, enhanced versions of this approach may offer promise for imaging tuberculosis in a clinical setting (30).

Evaluation of Therapeutic Efficacy with REF. After pulmonary infection with 10^6 CFU, we observed measurable fluorescent signal

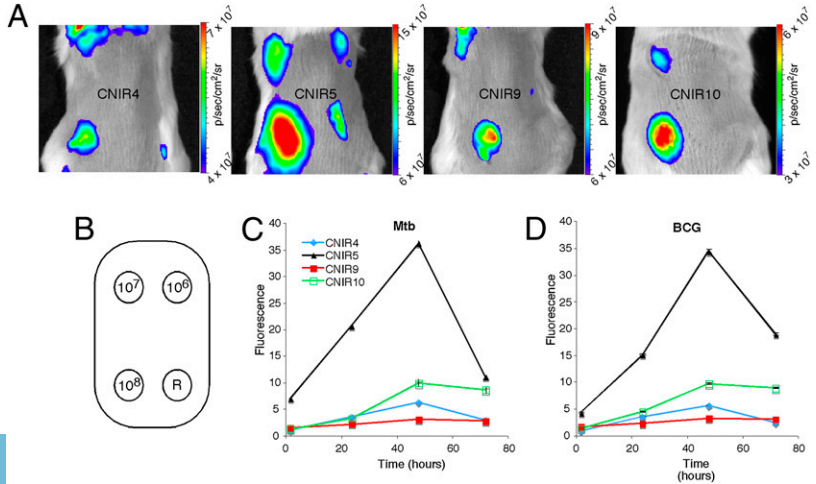

Fig. 4. Fluorogenic probes allow detection of *Mycobacterium tuberculosis* (Mtb) and bacillus Calmette–Guérin with similar sensitivity after s.c. infection. (*A*) Whole-body imaging of mice s.c. infected with Mtb and administered the indicated CNIR substrate. Images were taken 48 h postinfection and administration of the substrate. (*B*) Inoculation sites, number of bacteria present, and region of interest used for each animal. The position of the reference measurement is indicated (R). (*C*) Comparison of the signal as a function of time postinjection of each CNIR substrate for 10^8 Mtb or (*D*) bacillus Calmette–Guérin.

that normally increases and plateaus in signal intensity after the first 48 h postinfection. When rifampin and isoniazid (10 μg/mL each) are administered together either in vitro to bacteria alone or to infected mice, we observed a significantly different ($P < 0.01$) signal from the untreated controls within 24–48 h posttreatment (Fig. S3). These observations confirm that REF allows rapid evaluation of therapeutic efficacy either under laboratory conditions or during infections in mice.

Discussion

Endogenous enzymes combined with custom substrates allow sensitive detection of bacterial infection directly in living mice, as demonstrated by our use of REF for Mtb. The high sensitivity of this approach is due to a combination of the fact that the substrate does not need to gain access to the bacterial cytoplasm—only to the surface-localized BlaC enzyme—and the fluorescent product can build up at the site of infection, enhancing signal. Previous microarray studies indicate that BlaC is expressed constitutively by Mtb in vivo after more than 28 d postinfection in BALB/c and SCID mice (31) and at least 30 d postinfection in the Wayne model of nonreplicating persistence (32), suggesting that BlaC will make a good reporter under most in vivo-relevant conditions. Given that fluorogenic substrates can be developed for numerous enzymes, including proteases, kinases, ureases, β-galactosidases, and β-lactamases, REF technology should have utility for detection and imaging of many pathogens. The stability of the fluorescent product ensures proper localization to infected tissue and the ability to follow the site of infection in real time. This system displays promise for use in detecting infection in patients where bacteria cannot be tagged with conventional reporters before imaging and diagnosis.

Probes for bacteria that use catalytic enzymes, as in the case of REF, are likely to be very sensitive because they are not limited by the number of tagged molecules that can be delivered to the site of infection as compared with background, but continuously produce more signal as long as substrate is available. Use of a natural enzyme that is not expressed by the host ensures specificity and prevents potential metabolic impacts due to heterologous gene expression. The value of using endogenous systems for imaging is supported by studies using thymidine kinase for SPECT (33), but

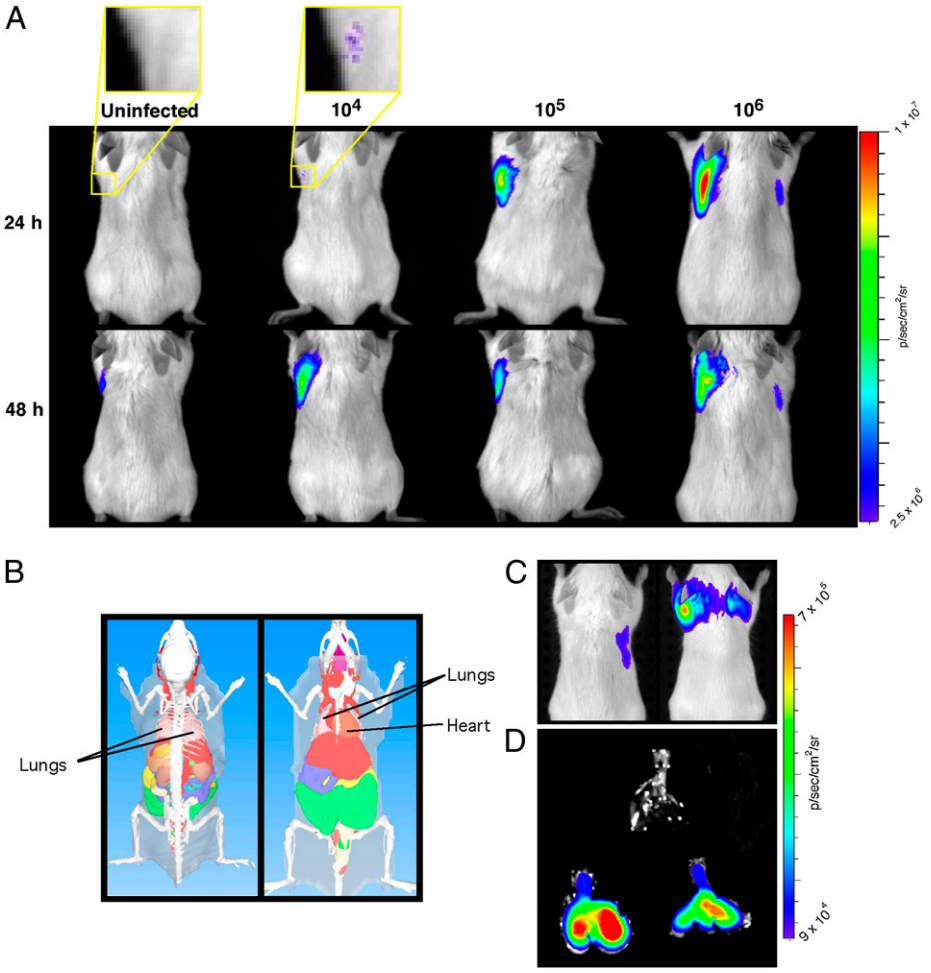

Fig. 5. Fluorogenic probes allow detection of bacillus Calmette–Guérin and *Mycobacterium tuberculosis* (Mtb) after pulmonary infection of mice. (*A*) Signal levels from mice infected with bacillus Calmette–Guérin by the pulmonary route of inoculation that were administered CNIR5 immediately after infection or uninfected mice that were also administered CNIR5. The yellow boxes within the first two mouse image panels indicate the regions that were magnified fourfold to produce the images above the mouse image panels. (*B*) Depiction of dorsal and ventral views of a mouse with organs to provide the anatomical context for the observed signal. (*C*) Whole-body images using transillumination after pulmonary infection with Mtb in mice in the same manner as in *A*. The mouse on the left is uninfected but was administered the CNIR5 substrate whereas the mouse on the right is infected with Mtb by aerosol and was administered CNIR5 immediately after infection. Images were collected at 48 h postinfection with administration of CNIR5 at the same time as infection. (*D*) Lungs were harvested from infected (lower two sets of lungs) and uninfected (top lungs) animals immediately after live animal images were collected. Lungs were harvested postmortem from the same animals that were first imaged alive (*C*), and then the lungs themselves were imaged (*D*). The CFU means and SD of four mice for each dose were (*A*) $1.3 \pm 0.6 \times 10^4$, $1.1 \pm 0.02 \times 10^5$, and $1.0 \pm 0.2 \times 10^6$ and (*C* and *D*) $1.0 \pm 0.6 \times 10^6$.

thymidine kinase-based imaging is not an option for clinical mycobacteria because they do not produce this enzyme and a recombinant strain is required (9, 10). An additional benefit of BlaC as an endogenous reporter is the fact that it is available outside the bacterial cell. The conclusion that the Mtb BlaC is surface-localized after secretion is consistent with observations that β-lactamase activity is associated with the surface in mycobacteria (15, 34, 35). The fact that BlaC is surface-localized and expressed in all Mtb allows the fluorescent product to provide bacterial location without the need for the substrate to cross the bacterial membrane. Hence, the sensitivity of this strategy allows quantitative detection of Mtb both under laboratory conditions and during animal infections.

The potential uses of this technology to facilitate tuberculosis research are nearly limitless. We demonstrate labeling of the bacteria, quantitative assessment of host cell infection, identification of infected cells by both microscopy and FACS, detection of Mtb in animals, quantitative analysis of infection, and localization to specific tissues. The nearly linear correlation between bacterial numbers and fluorescence signal indicates that REF is well suited for quantitative analysis of bacterial load during experiments where colony-forming units are commonly used and in animal tissues during infection or challenge studies. Because evaluation of Mtb bacterial numbers normally requires 3 wk or more, an immediate readout will have a profound impact on the Mtb field. Furthermore, considering the high sensitivity observed for mice, this approach should be applicable to other animal models, including rabbits and guinea pigs (36–40). Even if REF were used in combination with colony-forming units, having information that would allow experiments to be repeated or revised on the basis of the REF data before obtaining the CFU data would greatly speed progress.

Our study demonstrates that Mtb can be detected and quantified in living mice using custom fluorescent substrates for endogenous β-lactamase, which allows detailed real-time analysis of pulmonary infections. Because BlaC is expressed by all Mtb strains examined, it is likely that REF can be directly applied to clinical strains and other pathogenic mycobacteria because it utilizes a naturally produced enzyme for detection. Although the half-life for β-lactamases can vary somewhat (41), it has been estimated at around 206 min in mammalian cells (22), suggesting that enzyme levels represent a reasonable surrogate for numbers of viable bacteria. This assertion is supported by the strong correlation that we observed between viable bacterial numbers and REF signal in vitro and in animals (Fig. 3*A* and Fig. S2*D*). Thus, REF allows real-time estimation of the bacterial load in tissues, a key measure of virulence for attenuated mutants, efficacy of vaccines, and antimicrobial therapeutic potential. Our observation that therapeutics can be evaluated within 24–48 h with REF supports this conclusion. The presence of β-lactamases in bacteria, such as *P. aeruginosa* or methicillin-resistant *S. aureus*, that cause community-acquired pneumonias (CAP) could potentially interfere with REF, but the clinical presentation for tuberculosis is frequently sufficiently different from CAP (42–46) that the typical nodular lesions in the apical lobe of the lung found with tuberculosis are more likely to be misdiagnosed as carcinoma (46–48). Carcinoma could be differentiated from tuberculosis using REF imaging, making REF a potentially valuable tool in the diagnostic arsenal. Because the Mtb BlaC enzyme has a relatively unique active site pocket (21), studies are ongoing to further optimize the structure of our custom probes to produce even more highly sensitive and specific detection and imaging of Mtb in animals with the hope of ultimately applying this technology directly to tuberculosis patients. This tool will also facilitate tuberculosis research through accelerating progress toward development of diagnostics, vaccines, and therapeutics.

Materials and Methods

Strains and Growth Conditions. With the exception of Fig. 1 where multiple strains were used, Mtb strain Erdman was used for all experiments. All strains were grown as described previously (49). Bacterial numbers were confirmed in all experiments by plating dilutions for colony-forming units. Additional details are included in *SI Materials and Methods*.

Cell Lines and Culture Conditions. The murine macrophage cell line J774A.1 (ATCC TIB67) was maintained at 37 °C and 5% CO_2 in high glucose Dulbecco's Modified Eagle Medium (DMEM; Gibco) supplemented with 10% heat-inactivated FBS (Gibco) and 2 mM L-glutamine.

Macrophage Infection Assays. J774A.1 cells were infected as described previously (50). Additional details are included in *SI Materials and Methods*.

Flow Cytometry. Mtb strain CDC1551 was transformed with the vector pFJS8 that carries the L5 promoter expressing GFP (51). Flow cytometry was conducted essentially as described previously (52). Additional details are included in *SI Materials and Methods*.

Mouse Infections. Infections were by intratracheal instillation of 10^4–10^6 CFU to the lungs (53) for bacillus Calmette–Guérin and aerosol using the Madison chamber (52) for Mtb. Comparable imaging and bacterial viability data were obtained with either route. Additional details are included in *SI Materials and Methods*. Animal use protocols were reviewed and approved by the Institutional Animal Care and Use Committee of Texas A&M University.

β-Lactamase Activity Assays and Fractionation. Cultures of mycobacteria grown to early exponential phase (OD_{600} = 0.4) and centrifuged for 10 min at 3,000 × *g* to separate the bacteria from the supernatant. The supernatant was filtered through a 0.45-μm filter and retained as the culture filtrate. The pellet was washed twice with sterile PBS and resuspended to the original volume in PBS (whole-cell fraction). A portion of the whole-cell fraction was lysed by sonication with 30-s pulses at 60% output over 6 min on ice (crude lysate). The crude lysate was centrifuged for 30 min at 20,000 × *g* at 4 °C, and the pellet was resuspended in an equal volume of PBS (membrane fraction). Volumes of each fraction equivalent to 10^7 bacteria were aliquoted into 96-well plates for assays. Fluorocillin Green (Invitrogen) was added at 4.5 μM to each well, and the plates were shaken gently for 5 min at room temperature and incubated at 37 °C between 30 min and 20 h. The change in fluorescence was measured by excitation at 485 nm and emission at 530 nm.

Design and Synthesis of β-Lactamase Imaging Probes. The general principle for probe design is FRET. Each probe contains the lactam component that will be recognized by β-lactamase, a fluorescent group, and a light absorber. Because of the FRET-based quenching effect, they are initially at the quenched or dark state when the fluorescent group is excited. β-Lactamase cleavage of the lactam ring triggers spontaneous fragmentation that releases the light absorber connected to the 3′ position of the lactam from the fluorescent group, thus breaking the FRET process and leading to fluorescence emission. Two near-infrared cyanine dyes (Cy5, Cy5.5) were chosen due to their long emission wavelength that is suitable for in vivo fluorescence imaging. Correspondingly, we modified the nonemitting dye QSY21 as the quenching group in the probe into a hydrophilic QSY21 disulfonate that absorbs maximally at 649 nm and a hydrophobic QSY22 that absorbs maximally at 670 nm. Both were paired with Cy5 or Cy5.5 to make four probes, designated CNIR4, CNIR5, CNIR9, and CNIR10. CNIR5 is very stable in PBS, with a spontaneous hydrolysis rate of $1.75 \times 10^{-7} \cdot s^{-1}$. The enzymatic acceleration is 3.36×10^6. All probes display good solubility in aqueous solutions due to the sulfonate groups present. CNIR5 is soluble to at least 100 μM in water. All probes were prepared through multiple-step organic syntheses, purified by reverse-phase HPLC, and validated by matrix-assisted laser desorption/ionization time-of-flight mass spectrometry. Additional details for synthesis are included in *SI Materials and Methods*.

Imaging Tuberculosis Infections. Mice were anesthetized with isofluorane and imaged in an IVIS Spectrum (Caliper Life Sciences) with and without filters for fluorescence. Images were analyzed with Living Image Software v3.1 using spectral unmixing algorithms to remove autofluorescence, with one of the resulting channels locked to fit the emission spectrum of the appropriate fluorophore (Cy5 or Cy5.5). Representative images were randomly selected from images of four mice for all figures. Additional details are included in *SI Materials and Methods*.

Confocal Fluorescence Microscopy. Cells were seeded in 8-well chamber slides with 1×10^5 cells per well in 200 μL of DMEM plus 10% FBS overnight at 37 °C in 5% CO_2. The medium was removed, and GFP expressing Mtb was added to each well at an MOI of 10 (bacteria per cell) in 200 μl of medium. The bacteria were coincubated with the cells for 30 min and washed twice with PBS to remove extracellular bacteria, and medium plus 200 μg/mL amikacin was added for 2 h at 37 °C to select for intracellular bacteria. The cells were washed twice with PBS and placed in medium plus 20 nM substrate for 24 h at 37 °C in 5% CO_2 and washed twice with PBS. The cells were stained with 10 μg/mL DAPI, washed twice with PBS, and fixed in 4% paraformaldehyde in PBS for 30 min at room temperature. After washing, the slides were dried and mounted for confocal fluorescence microscopy.

Statistical Analyses. All experiments were carried out in triplicate and repeated at least three times. The significance of the results was determined using the Student's *t* test or ANOVA, as needed. $P < 0.05$ was considered significant.

ACKNOWLEDGMENTS. This work was supported by Grant 48523 from the Bill & Melinda Gates Foundation and by Grant AI47866 from the National Institutes of Health.

1. Dye C, et al. (2008) Measuring tuberculosis burden, trends, and the impact of control programmes. *Lancet Infect Dis* 8:233–243.
2. Kim DH, et al. (2008) Treatment outcomes and long-term survival in patients with extensively drug-resistant tuberculosis. *Am J Respir Crit Care Med* 178:1075–1082.
3. Dorman SE, Chaisson RE (2007) From magic bullets back to the magic mountain: The rise of extensively drug-resistant tuberculosis. *Nat Med* 13:295–298.
4. Heuts F, Carow B, Wigzell H, Rottenberg ME (2009) Use of non-invasive bioluminescent imaging to assess mycobacterial dissemination in mice, treatment with bactericidal drugs and protective immunity. *Microbes Infect* 11:1114–1121.
5. Hickey MJ, et al. (1996) Luciferase in vivo expression technology: Use of recombinant mycobacterial reporter strains to evaluate antimycobacterial activity in mice. *Antimicrob Agents Chemother* 40:400–407.
6. Arain TM, Resconi AE, Hickey MJ, Stover CK (1996) Bioluminescence screening in vitro (Bio-Siv) assays for high-volume antimycobacterial drug discovery. *Antimicrob Agents Chemother* 40:1536–1541.
7. Andrew PW, Roberts IS (1993) Construction of a bioluminescent mycobacterium and its use for assay of antimycobacterial agents. *J Clin Microbiol* 31:2251–2254.
8. Cooksey RC, Crawford JT, Jacobs WR, Jr, Shinnick TM (1993) A rapid method for screening antimicrobial agents for activities against a strain of Mycobacterium tuberculosis expressing firefly luciferase. *Antimicrob Agents Chemother* 37:1348–1352.
9. Davis SL, et al. (2009) Bacterial thymidine kinase as a non-invasive imaging reporter for Mycobacterium tuberculosis in live animals. *PLoS ONE* 4:e6297.
10. Davis SL, et al. (2009) Noninvasive pulmonary [^{18}F]-2-fluoro-deoxy-D-glucose positron emission tomography correlates with bactericidal activity of tuberculosis drug treatment. *Antimicrob Agents Chemother* 53:4879–4884.
11. Wendland M, Bumann D (2002) Optimization of GFP levels for analyzing Salmonella gene expression during an infection. *FEBS Lett* 521:105–108.
12. Rang C, Galen JE, Kaper JB, Chao L (2003) Fitness cost of the green fluorescent protein in gastrointestinal bacteria. *Can J Microbiol* 49:531–537.
13. Coulson NM, Fulop M, Titball RW (1994) Effect of different plasmids on colonization of mouse tissues by the aromatic amino acid dependent Salmonella typhimurium SL 3261. *Microb Pathog* 16:305–311.
14. Hugonnet JE, Tremblay LW, Boshoff HI, Barry CE, III, Blanchard JS (2009) Meropenem-clavulanate is effective against extensively drug-resistant Mycobacterium tuberculosis. *Science* 323:1215–1218.
15. Flores AR, Parsons LM, Pavelka MS, Jr. (2005) Genetic analysis of the beta-lactamases of Mycobacterium tuberculosis and Mycobacterium smegmatis and susceptibility to beta-lactam antibiotics. *Microbiology* 151:521–532.
16. Weissleder R, Tung CH, Mahmood U, Bogdanov A, Jr. (1999) In vivo imaging of tumors with protease-activated near-infrared fluorescent probes. *Nat Biotechnol* 17:375–378.
17. Knox JR, Moews PC, Frere JM (1996) Molecular evolution of bacterial beta-lactam resistance. *Chem Biol* 3:937–947.
18. Hermann JC, Ridder L, Höltje HD, Mulholland AJ (2006) Molecular mechanisms of antibiotic resistance: QM/MM modelling of deacylation in a class A beta-lactamase. *Org Biomol Chem* 4:206–210.
19. Davies J (1994) Inactivation of antibiotics and the dissemination of resistance genes. *Science* 264:375–382.
20. Fisher JF, Mobashery S (2009) Three decades of the class A beta-lactamase acyl-enzyme. *Curr Protein Pept Sci* 10:401–407.
21. Wang F, Cassidy C, Sacchettini JC (2006) Crystal structure and activity studies of the Mycobacterium tuberculosis beta-lactamase reveal its critical role in resistance to beta-lactam antibiotics. *Antimicrob Agents Chemother* 50:2762–2771.
22. Zlokarnik G, et al. (1998) Quantitation of transcription and clonal selection of single living cells with beta-lactamase as reporter. *Science* 279:84–88.
23. Campbell RE (2004) Realization of beta-lactamase as a versatile fluorogenic reporter. *Trends Biotechnol* 22:208–211.
24. Flores AR, Parsons LM, Pavelka MS, Jr (2005) Characterization of novel Mycobacterium tuberculosis and Mycobacterium smegmatis mutants hypersusceptible to beta-lactam antibiotics. *J Bacteriol* 187:1892–1900.
25. Xing B, Khanamiryan A, Rao J (2005) Cell-permeable near-infrared fluorogenic substrates for imaging beta-lactamase activity. *J Am Chem Soc* 127:4158–4159.
26. Weissleder R (2001) A clearer vision for in vivo imaging. *Nat Biotechnol* 19:316–317.
27. Cirillo SLG, Bermudez LE, El-Etr SH, Duhamel GE, Cirillo JD (2001) *Legionella pneumophila* entry gene *rtxA* is involved in virulence. *Infect Immun* 69:508–517.
28. Ntziachristos V, Ripoll J, Weissleder R (2002) Would near-infrared fluorescence signals propagate through large human organs for clinical studies? *Opt Lett* 27:333–335.
29. Ntziachristos V, Ripoll J, Weissleder R (2002) Would near-infrared fluorescence signals propagate through large human organs for clinical studies? Errata. *Opt Lett* 27:1652.
30. Ntziachristos V, Bremer C, Weissleder R (2003) Fluorescence imaging with near-infrared light: New technological advances that enable in vivo molecular imaging. *Eur Radiol* 13:195–208.
31. Talaat AM, Lyons R, Howard ST, Johnston SA (2004) The temporal expression profile of Mycobacterium tuberculosis infection in mice. *Proc Natl Acad Sci USA* 101:4602–4607.
32. Voskuil MI, Visconti KC, Schoolnik GK (2004) Mycobacterium tuberculosis gene expression during adaptation to stationary phase and low-oxygen dormancy. *Tuberculosis (Edinb)* 84:218–227.
33. Bettegowda C, et al. (2005) Imaging bacterial infections with radiolabeled 1-(2′-deoxy-2′-fluoro-beta-D-arabinofuranosyl)-5-iodouracil. *Proc Natl Acad Sci USA* 102: 1145–1150.
34. Zhang Y, Steingrube VA, Wallace RJ, Jr (1992) beta-Lactamase inhibitors and the inducibility of the beta-lactamase of Mycobacterium tuberculosis. *Am Rev Respir Dis* 145:657–660.
35. Fattorini L, et al. (1991) Beta-lactamase of Mycobacterium fortuitum: Kinetics of production and relationship with resistance to beta-lactam antibiotics. *Antimicrob Agents Chemother* 35:1760–1764.
36. Manabe YC, et al. (2008) The aerosol rabbit model of TB latency, reactivation and immune reconstitution inflammatory syndrome. *Tuberculosis (Edinb)* 88:187–196.
37. Converse PJ, et al. (2009) Role of the dosR-dosS two-component regulatory system in Mycobacterium tuberculosis virulence in three animal models. *Infect Immun* 77: 1230–1237.
38. Flynn JL (2006) Lessons from experimental Mycobacterium tuberculosis infections. *Microbes Infect* 8:1179–1188.
39. Orme IM (2003) The mouse as a useful model of tuberculosis. *Tuberculosis (Edinb)* 83: 112–115.
40. McMurray DN, et al. (2005) Vaccine-induced cytokine responses in a guinea pig model of pulmonary tuberculosis. *Tuberculosis (Edinb)* 85:295–301.
41. Matagne A, et al. (1990) The diversity of the catalytic properties of class A beta-lactamases. *Biochem J* 265:131–146.
42. Eddy OL (2005) Community-acquired pneumonia: From common pathogens to emerging resistance. *Emergency Medicine Practice* 7:1–24.
43. Kejariwal D, Sarkar N, Chakraborti SK, Agarwal V, Roy S (2001) Pyrexia of unknown origin: A prospective study of 100 cases. *J Postgrad Med* 47:104–107.
44. Fauci AS, et al. (2008) *Harrison's Principles of Internal Medicine* (McGraw Hill, New York), 17 Ed.
45. Harkirat S, Anand SS, Indrajit IK, Dash AK (2008) Pictorial essay: PET/CT in tuberculosis. *Indian J Radiol Imaging* 18:141–147.
46. Burrill J, et al. (2007) Tuberculosis: A radiologic review. *Radiographics* 27:1255–1273.
47. Lillington GA, Caskey CI (1993) Evaluation and management of solitary and multiple pulmonary nodules. *Clin Chest Med* 14:111–119.
48. Hara T, Kosaka N, Suzuki T, Kudo K, Niino H (2003) Uptake rates of ^{18}F-fluorodeoxyglucose and ^{11}C-choline in lung cancer and pulmonary tuberculosis: A positron emission tomography study. *Chest* 124:893–901.
49. Cirillo SL, et al. (2009) Protection of Mycobacterium tuberculosis from reactive oxygen species conferred by the mel2 locus impacts persistence and dissemination. *Infect Immun* 77:2557–2567.
50. Subbian S, Mehta PK, Cirillo SL, Bermudez LE, Cirillo JD (2007) A *Mycobacterium marinum mel2* mutant is defective for growth in macrophages that produce reactive oxygen and reactive nitrogen species. *Infect Immun* 75:127–134.
51. Wagner D, Sangari FJ, Kim S, Petrofsky M, Bermudez LE (2002) Mycobacterium avium infection of macrophages results in progressive suppression of interleukin-12 production in vitro and in vivo. *J Leukoc Biol* 71:80–88.
52. Khounlotham M, Subbian S, Smith R, III, Cirillo SL, Cirillo JD (2009) Mycobacterium tuberculosis interferes with the response to infection by inducing the host EphA2 receptor. *J Infect Dis* 199:1797–1806.
53. Cohen MK, Bartow RA, Mintzer CL, McMurray DN (1987) Effects of diet and genetics on *Mycobacterium bovis* BCG vaccine efficacy in inbred guinea pigs. *Infect Immun* 55: 314–319.